

Reaction-Advection-Diffusion Models of Air Pollution

Daniel Henricks

April 28, 2024

1 Introduction

Airborne pollutants are the single most impactful environmental risk to human health, with about one in nine deaths worldwide attributed to air pollution (Cohen et al., 2017). Poor air quality can cause many negative implications to human health; exposure to more air pollution is directly correlated to an increased rate of heart attacks and asthma. There are a few different types of air pollution that can cause adverse affects on human health. First, fine particulate matter ($\text{PM}_{2.5}$) causes approximately 95% of the deaths due to air pollution. ($\text{PM}_{2.5}$) is defined to be any microscopic particles that are of diameter of less than $2.5\mu\text{m}$, about 20 times smaller than the diameter of a human hair.

Due to the minute scale of these particles, particulate matter is capable of traveling deep into vital organs such as the lungs or the bloodstream. Exposure to increased rates of fine particulate matter can lead to coughing and difficulty breathing. Particulate matter is typically produced by the combustion of gasoline, oil, or wood, but has recently been discovered to occur at smaller rates from natural processes such as volcanic eruptions (Thangavel et al., 2022). In addition to particulate matter, surface-level ozone (O_3) and nitrogen dioxide (NO_2) also contribute to the damages to human health from air pollution. In this paper, we will validate recent diffusion models of air pollution and the models to estimate damages to human health caused by pollution.

2 Types of Models

Before beginning on the mathematics behind a differential equation model of air pollution, we will discuss how to form a model of air pollution. One of the main problems with making a diffusion model for air pollution is estimating the flux term of the diffusion equation. We apply Fick's first and second laws of diffusion; recall that Fick's first law relates the flux, J to the diffusion constant k , and the change in the concentration gradient c :

$$J = -k \frac{dc}{dx} \tag{1}$$

Typically, chemical transport models (CTMs), programs that simulate and predict atmospheric chemistry, are used to find the fluxes needed in a diffusion equation. There are two classes of CTMs: Eulerian and Lagrangian. Eulerian models have an observer standing in one location who is watching the air pass by, whereas the Lagrangian models have the observer moving along with the parcel of air as it takes a random walk through the atmosphere (Vallero, 2021).

However, executing CTMs can be computationally difficult. We will first look at a simple model for representing the concentrations of chemicals in the atmosphere.

2.1 A Simple Model

The model we will first investigate is called the one-box model (Jacob, 1999).

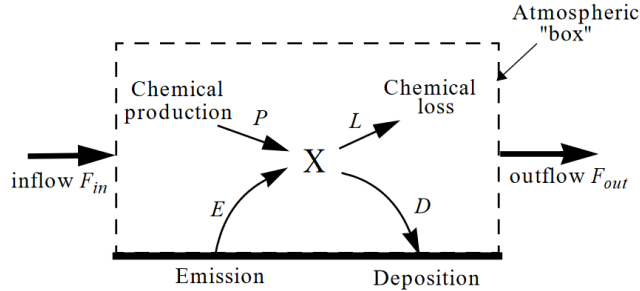


Figure 1: One-box model for an atmospheric species X

The one-box model for an atmospheric species X is illustrated in Figure 2. The model describes the concentration of X inside of some subset of the global atmosphere (ex: the United States). The transport rate is described using the flow in, F_{in} , and the flow out of, F_{out} of the box. By conservation, the global atmosphere must obey

$$F_{in} = F_{out} = 0$$

The other parameters of the model are:

- Chemical production (P)
- Emissions (E)
- Chemical loss (L)
- Deposition (D)

We will now define the lifetime, τ , of a molecule, to be the average time a molecule of X remains in our box. This will be the mass of the particle divided by the outflow of the box:

$$\tau = \frac{m}{F_{out} + L + D} \quad (2)$$

We also can set up a mass balance differential equation. The change of the abundance of a species must be equal to the sources less the sinks:

$$\frac{dm}{dt} = F_{in} + E + P - F_{out} - L - D \quad (3)$$

We need to represent the sinks using some loss rate. Let's assume that the losses are proportional to the amount of the species in the box, so the losses are equal to km . (It turns out trivially that $k = \frac{1}{\tau}$). Let's also assume that the sources are independent of m and are equal to some constant S . Then, we yield the ODE

$$\frac{dm}{dt} = S - km \quad (4)$$

which can be solved quite simply via separation of variables:

$$\begin{aligned} \frac{dm}{dt} &= S - km \\ \Rightarrow \int_0^t \frac{dm}{S - km} &= \int_0^t dt \\ \Rightarrow \frac{-1}{k} \ln \left| \frac{S - km(t)}{S - km(0)} \right| &= t \\ \Rightarrow S - km(t) &= S e^{-kt} - km(0) e^{-kt} \\ \Rightarrow m(t) &= \frac{S}{k} (1 - e^{-kt}) + m(0) e^{-kt} \end{aligned} \quad (5)$$

Finding the steady state of this equation yields $S_\infty = \frac{S}{k}$ (via taking the limit as $t \rightarrow \infty$).

This steady state assumption is reasonable because the rate of change of the mass, $\frac{dm}{dt}$, tends to be very small in comparison to the production rate. Because of this, we classify this steady state as a quasi steady state.

2.2 A More Realistic Model: the Puff Model

We will now investigate a puff model; such a model describes fluid elements moving in space. Note that the puff model is an example of a Lagrangian model (as mentioned above). We define a fluid element to be a volume of air in which all particles move with the same velocity. The most common application of a puff model is diffusion from a smokestack, something that is essential for understanding how air pollution diffusion. We define the mass balance equation for this model to be

$$\frac{dX_c}{dt} = E + P - L - D \quad (6)$$

where X_c is the concentration of element X. Assume that the puff takes a column shape and that the height of the column is h . Also assume that there is no chemical production (P) and that the losses are proportional to the concentration at some rate $L = kX_c$. We then form the mass-balance equation:

$$\frac{dX_c}{dt} = \frac{E}{h} - kX_c \quad (7)$$

This is another separable ODE which is trivial to solve. The puff model's steady states are only valid in low-wind conditions, however (Zannetti, 1985). Many computer systems used by the federal government to predict air pollution use variations of this model with more complicated parameters.

3 A first diffusion model

We will first review the diffusion model established by Tirabassi (1989). Analytical models such as this one use solutions to the advection-diffusion equation below:

$$u \frac{\partial C}{\partial x} = \frac{\partial}{\partial y} (K_y \frac{\partial C}{\partial y}) + \frac{\partial}{\partial z} (K_z \frac{\partial C}{\partial z}) + S \quad (8)$$

where the parameters are:

- Mean wind velocity (u)
- Concentration (C)
- Source term (S)
- Lateral eddy exchange constant (K_y)
- Vertical eddy exchange constant (K_z)

This model was further improved by Buske et. al (2012). In this paper, the initial equation was revised to break the concentration into a three-dimensional problem as seen below:

$$u \frac{\partial c}{\partial x} + v \frac{\partial c}{\partial y} + w \frac{\partial c}{\partial z} = \frac{\partial}{\partial x} (K_x \frac{\partial c}{\partial x}) + \frac{\partial}{\partial y} (K_y \frac{\partial c}{\partial y}) + \frac{\partial}{\partial z} (K_z \frac{\partial c}{\partial z}) \quad (9)$$

This equation essentially states that the mean wind vector can be broken up into its components and that the suspended material must be conserved. We limit the domains of x , y , and z to $0 < x < L_x$, $0 < y < L_y$, and $0 < z < h$, where h is the height of the atmospheric boundary layer. We also impose a value of zero for the eddy diffusivities at the edges of the domain. Since the solution to the three-dimensional problem can be hard to find, we want to find a way to transform this equation to a two-dimensional problem. To do this, we need to transform the problem to one with variables x and z :

First, we create a complete set of orthogonal basis functions in the y-direction over the y-domain. Define

$$Y_m(y) = \cos(\lambda_m y)$$

and

$$\lambda_m = \frac{m\pi}{L_y}, m \in \mathbb{N}^+$$

From doing this, we have created a way for any function $f(y)$ to be represented as some linear combination of these eigenfunctions:

$$f(y) = \sum_{m=0}^{\infty} c_m Y_m(y)$$

We then plug in our unknown coefficient of two variables to get equation (4) in Buske (2012):

$$f(y) = \sum_{m=0}^{\infty} c_m(x, z) Y_m(y) \quad (10)$$

To find the value of this coefficient, we will first define some integrals. Let $Y_n(y)$ also be a orthogonal eigenfunction. Then we define

$$\begin{aligned} \int_0^{L_y} Y_m(y) Y_n(y) dy &= \alpha_{mn} \\ \int_0^{L_y} Y'_m(y) Y_n(y) dy &= \beta_{mn} \\ \int_0^{L_y} K_y Y_m(y) Y_n(y) dy &= \gamma_{mn} \\ \int_0^{L_y} K'_y Y'_m(y) Y_n(y) dy &= \eta_{mn} \end{aligned}$$

This will help simplify our derivation for finding the unknown constant $c_m(x, z)$.

We first take the chain rule of each of the terms in the diffusion equation and plug in our new equation for the concentration:

$$\frac{\partial}{\partial x} [K_x \frac{\partial c(x, y, z)}{\partial x}] = [\frac{\partial}{\partial x} (K_x \frac{\partial c(x, z)}{\partial x}) + K_x \frac{\partial^2 c(x, z)}{\partial x^2}] Y_m(y)$$

The same process is done for the y-derivative, yielding

$$K'_y c_m(x, z) Y'_m(y) + K_y \frac{\partial^2 c}{\partial y^2} c_m(x, z) \cos(\lambda_m y)$$

The z-derivative also follows the same process, which will be omitted for brevity. To put the equations into the form specified above, we evaluate the

derivatives and then move over the advection terms. Doing this yields, as shown briefly above,

$$[\frac{\partial}{\partial x}[K_x \frac{\partial c(x, z)}{\partial x}] + \frac{\partial}{\partial z}[K_z \frac{\partial c(x, z)}{\partial z}] - u \frac{\partial c(x, z)}{\partial x} - w \frac{\partial c(x, z)}{\partial z}] Y_m(y)$$

The rest of the terms in the equation come from the chain rule affects of the y derivative. The first term can be reorganized as

$$c_m(x, z) K'_y Y'_m(y)$$

and the second term as

$$c_m(x, z) K_y Y''_m(y)$$

where

$$Y''_m(y) = -\lambda_m^2 \cos(\lambda_m y) = -\lambda_m^2 Y_m(y)$$

Substituting, we get

$$-\lambda_m^2 c_m(x, z) K_y Y_m(y)$$

We have now completed most of the tedious algebra. We then can apply the operator $\int_0^{L_y} Y_n(y) dy$ to obtain the result

$$\begin{aligned} & \sum_{m=0}^{\infty} \left[\frac{\partial}{\partial x} \left(K_x \frac{\partial c(x, z)}{\partial x} \right) + \frac{\partial}{\partial z} \left(K_z \frac{\partial c(x, z)}{\partial z} \right) \right. \\ & \quad - u \frac{\partial c(x, z)}{\partial x} - w \frac{\partial c(x, z)}{\partial z} \alpha_{mn} \\ & \quad - v c_m(x, z) \beta_{mn} \\ & \quad - \lambda_m^2 c_m(x, z) \gamma_{mn} \\ & \quad \left. + c_m(x, z) \eta_{mn} \right] \end{aligned} \tag{11}$$

We now will make some assumptions to simplify this equation. In the ABL, it is common to treat the speeds v and w as zero, such as in Tirabassi (1989). We also assume that the force of advection is much more dominant than the force of diffusion in the x-direction. Mathematically, this is

$$u \frac{\partial c(x, z)}{\partial x} \gg \frac{\partial}{\partial x} (K_x \frac{\partial c(x, z)}{\partial x})$$

Because of this, we can neglect the diffusion component K_x . We also consider that K_y only depends on the z-direction.

We can now rewrite equation (11) above as:

$$u \frac{\partial c(x, z)}{\partial x} = \frac{\partial}{\partial z} (K_z \frac{\partial c(x, z)}{\partial z}) - \lambda_m^2 K_y c_m(x, z) \tag{12}$$

3.1 An interpretation of this result

This result turned out to be very accurate against experimental data (Buske, 2012). The equation shown above was ran against data from Copenhagen, Denmark, and Kinkaid, Illinois. The difference between the predicted and actual results turned out to be within an appropriate error bound, leading for the authors to conclude that analytical solutions to the advection differential equation (ADE) may be possible. The potential for creating an accurate and computationally efficient model for modeling air pollution dispersion encouraged more research into new methods of CTMs.

4 InMAP: A more computationally efficient model for finding emissions

One of the recent developments in the study of air pollution was the creation of computationally efficient models for computing the harm to human health from diffusion. A prevalent model that has been implemented in industry by companies such as WattTime is InMAP (<http://spatialmodel.com/>). InMAP is a model that evaluates pollution by simplifying typical CTMs via using an annual-average basis for its results. InMAP itself was based on a revolutionary CTM, WRF-Chem (Grell et al., 2005).

4.1 How does WRF-Chem work?

WRF-Chem is a CTM that is based on the Weather Research and Forecasting Model (WRF). The WRF was initially created by researchers in the late 1990s via a collaboration between the National Center for Atmospheric Research (NCAR), the National Oceanic and Atmospheric Administration, and many others. WRF is most useful for its capability to apply a mathematical model via a direct simulation with idealized conditions or use actual atmospheric data. It is used at many meteorological companies as well as in solar companies, laboratories, and many other locations.

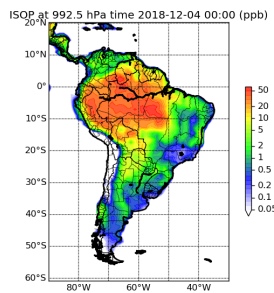


Figure 2: An example of the graphics produced by WRF Chem.

WRF-Chem combines this with the ability to trace $PM_{2.5}$. It is very numerically consistent and its forecasts are stronger than many models beforehand. However, like many other CTMs, WRF-Chem is very computationally expensive.

4.2 InMAP’s solutions

To solve many of the computational issues that WRF-Chem had, InMAP makes several key simplifications. InMAP simplifies many of the marginal emissions rates into annual averages, creating an algorithm that can be run much more efficiently. In addition to being more computationally efficient, InMAP also creates more spatially detailed results. This efficiency is achieved by using a variable-resolution grid: areas with a higher density of people are modeled with a higher spatial detail than regions of lower density. The algorithm is able to be downloaded and is programmed using the Go programming language; it is designed to be simple enough for a beginner user to learn. The authors claim that this is a novel approach to CTMs.

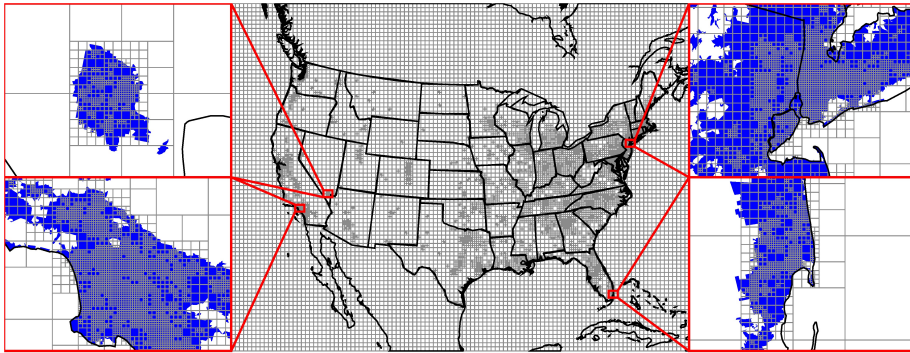


Figure 3: How InMAP splits the US into regions. Note how regions with higher population density are modeled as smaller grid regions, and regions with lower density have larger grid regions

4.3 The diffusion equation

InMAP utilizes a reaction-advection-diffusion equation to find its air pollution concentrations:

$$\frac{\partial C_i}{\partial t} = \underbrace{\nabla \cdot (D \nabla C_i)}_{\text{Diffusion Term}} - \underbrace{\nabla \cdot (\vec{v} C_i)}_{\text{Advection Term}} + \underbrace{\sum_{j=1}^n R_{ij}}_{\text{Reaction Terms}} + \underbrace{\sum E_i}_{\text{Source/Sink Term}} - \underbrace{\sum d_i}_{\text{Decay Term}} \quad (13)$$

where

- C_i is the concentration of one of n model pollutant species.
- D is a molecular diffusion coefficient (neglected here as a negligible source of chemical transport in the atmosphere compared to advection).
- \vec{v} is the wind vector.
- R_{ij} is the net formation rate of species i from species j .
- E_i is pollutant emission.
- d_i is pollutant removal via wet and dry deposition.

InMAP solves this equation for the concentrations of PM_{2.5} and many other harmful chemicals emitted. To find the concentrations, InMAP runs in each grid region at a discrete step interval. During each step, the following are performed:

1. InMAP finds the flux that comes from new emissions. This is done using the plume model, as referenced before.
2. The algorithm then calculates how changes in pollutant concentrations are affected by physical and chemical processes including advection, turbulent mixing, etc.
3. Each process listed above uses a snapshot of the concentration before the time step had occurred to avoid combining changes to concentrations at the same time.

4.4 How InMAP takes in data

InMAP first takes in the data and runs it through a preprocessor that is an extension of WRF-Chem. This reduces the complexity of the operations that need to be ran after. Since the CTM is computationally expensive to run, the input data time step is once per WRF-Chem simulation hour. After this, the InMAP algorithm runs stepwise, adjusting the relevant terms of the equation as needed. One of the more interesting features is the methodology of updating the advection wind vectors. The wind speed updates at too fast of a rate for any computer to calculate using discrete steps. To solve this problem, Reynolds decomposition is used: this is a mathematical technique that uses the expected value of a wind stream and its deviations to calculate an accurate result. For example, if a variable x is decomposed, it would be represented as the following equation:

$$x = \bar{x} + x' \quad (14)$$

where

- \bar{x} is the expected value of x
- x' is deviations in x .

InMAP does this process for calculating the wind velocity in the advection term of equation (13). InMAP splits each variable into three parts:

$$v = \bar{x} + \tilde{x} + v', C = \bar{C} + \tilde{C} + C' \quad (15)$$

where \tilde{x} and \tilde{C} are deviations calculated by WRF-Chem, and v' and C' are other deviations.

Substituting this decomposition into equation (13) yields:

$$\nabla \cdot (vC_i) = \nabla \cdot ((\bar{x} + \tilde{x} + x')(\bar{C}_i + \tilde{C}_i + C'_i))$$

$$= \nabla \cdot (\bar{x}\bar{C}_i) + \nabla \cdot (\bar{x}\tilde{C}_i) + \nabla \cdot (\bar{x}C'_i) + \nabla \cdot (\tilde{x}\bar{C}_i) + \nabla \cdot (\tilde{x}\tilde{C}_i) + \nabla \cdot (\tilde{x}C'_i) + \nabla \cdot (x'\bar{C}_i) + \nabla \cdot (x'\tilde{C}_i) + \nabla \cdot (x'C'_i)$$

We now apply the Reynolds averaging rules to remove four of the above terms to yield:

$$= \nabla \cdot (\bar{x}\bar{C}_i) + \nabla \cdot (\tilde{x}\tilde{C}_i) + \nabla \cdot (\tilde{x}C'_i) + \nabla \cdot (x'\tilde{C}_i) + \nabla \cdot (x'C'_i) \quad (16)$$

We now have to discretize the first term of the above equation. InMAP chooses to do that using the following equation:

$$\frac{\Delta C_i}{\Delta t} = \begin{cases} \frac{1}{\Delta x} \sum_{j=1}^{n_y} U_i C_{i,j} n_j, & \text{if } U_i \geq 0 \\ \frac{1}{\Delta x} \sum_{j=1}^{n_y} U_i C_{i,j}, & \text{if } U_i < 0 \end{cases}$$

We now have most of the required information verified to begin running InMAP. To demonstrate further, an example of the output of the algorithm is shown below:

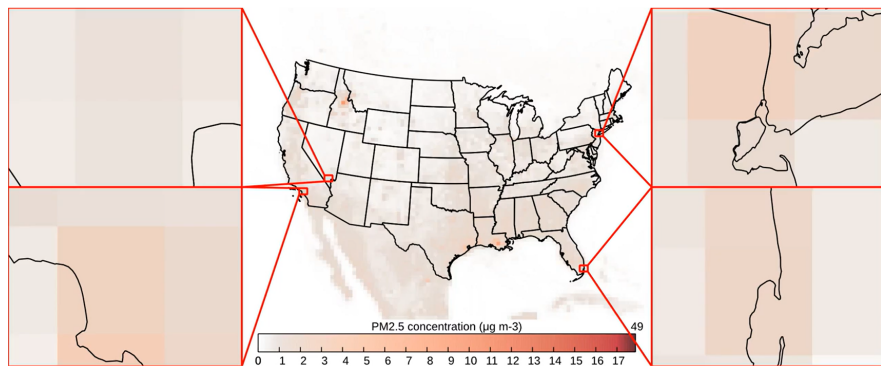


Figure 4: The result of the model when running with PM_{2.5} as the specified pollutant.

4.5 Configuring InMAP

InMAP allows the user to have lots of flexibility regarding configuring the model. After downloading the executable, the program prompts the user to provide a configuration file. Within this file, there exists many configuration options, some of which are shown below:

```
[OutputVariables]
TotalPM25 = "PrimaryPM25 + pNH4 + pSO4 + pNO3 + SOA"
TotalPopD = "(exp(log(1.078)/10 * TotalPM25) - 1) * TotalPop * allcause / 100000"
WhiteNoLatD = "(exp(log(1.078)/10 * TotalPM25) - 1) * WhiteNoLat * allcause / 100000"
BlackD = "(exp(log(1.078)/10 * TotalPM25) - 1) * Black * allcause / 100000"
NativeD = "(exp(log(1.078)/10 * TotalPM25) - 1) * Native * allcause / 100000"
AsianD = "(exp(log(1.078)/10 * TotalPM25) - 1) * Asian * allcause / 100000"
LatinoD = "(exp(log(1.078)/10 * TotalPM25) - 1) * Latino * allcause / 100000"
TotalPop = "TotalPop"
PrimPM25 = "PrimaryPM25"
PSO4 = "pSO4"
PNO3 = "pNO3"
PNH4 = "pNH4"
SOA = "SOA"
SOX = "SOX"
NH3 = "NH3"
NOx = "NOx"
BasePM25 = "BaselineTotalPM25"
WindSpeed = "WindSpeed"
```

Figure 5: A few of the configuration options available. The total PM_{2.5} concentration is composed of multiple sources. The total deaths per ethnicity are also shown.

The model can then be executed. The execution time of the model is still quite long, so it is easier to access InMAP via an API.

5 Results

To obtain our results, we utilized an API created by the company WattTime. WattTime combines marginal emission rates with InMAP’s results to produce a figure representing the health damage per MWh (using the actuarial values for a human life). To better understand how marginal emissions rates impact damage to human health caused by emissions, consider the states of California and Mississippi. California has a much cleaner grid with a higher access to renewable energy, so if a spike in demand occurs for energy production, it is much easier to compensate that demand with renewable energy. However, in Mississippi, only 3 percent of the energy produced is renewable. In addition, the state consumes three times more energy than it produces. These factors make the marginal emissions rates in Mississippi much higher than ones in California.

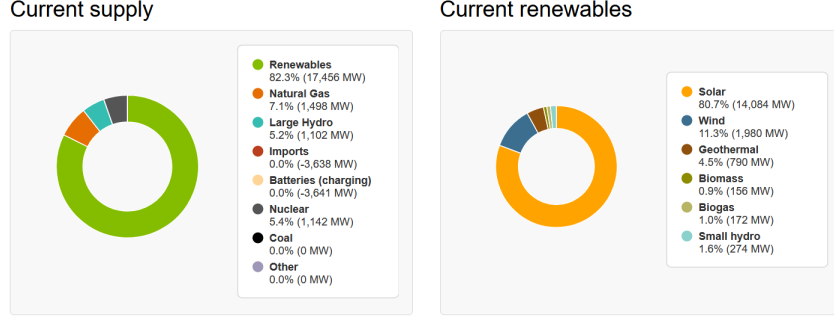


Figure 6: A snapshot of California’s grid makeup according to CAISO, California’s Independent System Operator.

5.1 Pricing of energy and marginal operating emissions rates (MOERs).

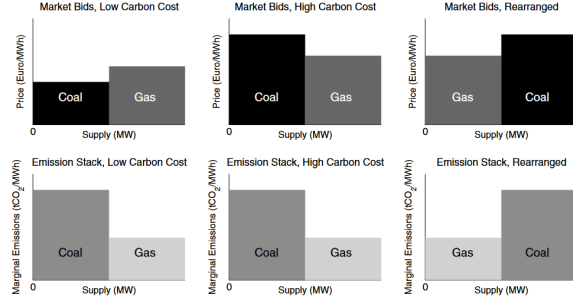


Figure 7: Consider a simple market with one coal generator and one gas generator. Initially, the cost of carbon is low, and bids from coal generators are cheaper than those from gas generators. As emissions become more costly, the cost of producing coal becomes more expensive than the cost of producing gas. The result of the higher allowance price is lower emissions, as intended. (Howison, 2012)

For energy to be a traded commodity, electricity markets have to be deregulated. Some of the first markets to do this were Alberta, Canada, which was deregulated in January of 1996, and California, which was deregulated in April 1998 (Barlow, 2002). One of the strange features of power markets is the fact that zero or negative energy prices can occur and that the variance of prices is much higher than other markets. In California, power usage peaks in the summer, whereas in Alberta, power usage and prices peak in the winter (due to the cold). Since the energy markets are still relatively new, many papers rely

on the early assumption that energy prices follow a diffusion model. One of the key factors of this model is the fact that the price of energy can spike at times when demand is much larger than supply.

Historically, in the absence of the trading of renewable energy credits (RECs), more pollution-intensive fuels are the first to be used when an increase in power is demanded (Howison, 2012), meaning that the marginal emissions rate is higher when there is no incentives to use renewable energy. Therefore, in areas where the cost of producing an additional unit of nonrenewable energy is much smaller than the cost of producing renewable energy, the average marginal emissions rate will be higher. This explains why there is such a large difference in the MOER between regions of the United States.

To better visualize the emissions in the United States, WattTime provides a GeoJSON file of all of the Balancing Authorities in the United States. In each of these regions, a marginal emissions rate is calculated every five minutes. Marginal emissions rates can range from about 600 pounds of carbon produced per megawatt-hour in less carbon intense regions to over 2,000 pounds of carbon in more carbon intense grids. Using Leaflet (a JavaScript library used to visualize maps), the following map was created:

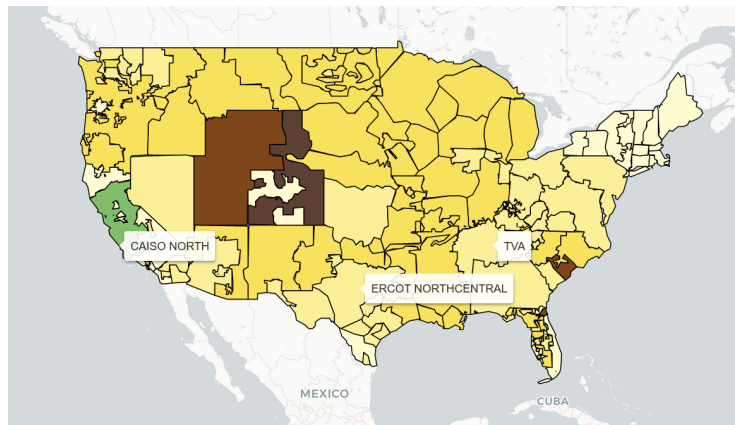


Figure 8: A map of all the Balancing Authorities (BAs) in the United States. Areas with higher marginal emissions rates (colored in brown/dark brown) will have higher health damages due to air pollution due to a higher reliance on non-renewable sources. Conversely, areas with a lower MOER (colored in green/light yellow) will have lower health damages due to air pollution.

Now, we have to combine this marginal emissions rate with the InMAP model. Luckily, WattTime already has an API endpoint that does this. Using the same methods as before, we can create a map of selected Balancing Authorities and their respective health damages per MWh.

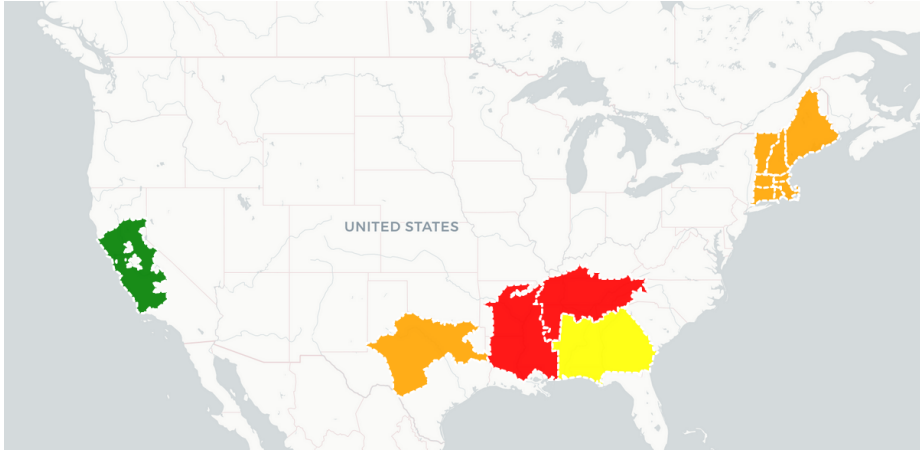


Figure 9: A map of selected health damages in the United States. Red colors mean higher health damage, whereas green colors correspond to lower health damage. As of April 28th, 2024, at 4:30 PM CDT, the TVA region had a damage to human health of \$45.70 per MWh of energy produced versus a damage to human health of \$1.00 in California per MWh.

5.2 Final results and statistics

WattTime also provides historical health damages for most locations in the United States since 2022. Using a running average from January 1st, 2024, to April 1st, 2024, we created a Python script to compute the average health damage per region.

Table 1: Average Health Damage and MOER by Region for January 1 to April 1, 2024

Region	Health Damage	MOER
TVA (Tennessee, Mississippi)	\$54.00	1,171
MISO Lower MS River (Louisiana, Arkansas)	\$60.60	1,389
CAISO NORTH (California)	\$10.50	718

Some interesting statistics we can get from this are:

1. The health damages in areas with higher poverty rates tend to be greater than in those with more wealth.
2. Solar farms typically have a lifespan of 35-40 years. Assuming a lifespan of 40 years with no downtime due to operational errors, building 1 MW of solar energy in the TVA region will produce approximately 80,000 MWh of energy (see <https://clearloop.us/tn-paris/>). With an average health

damage of \$54.00, the social benefit of building this solar farm will be approximately \$4,320,000.

3. The average health damage in the selected Southeastern regions is over five times greater than that in California.

6 Conclusion

In this paper, we have explained how air pollution can be one of the most detrimental factors to human health. Through the verification of various ordinary differential equation models, in addition to diffusion and advection models for air pollution, the foundations of InMAP were explained. In addition, recent experimental data on air pollution was utilized to prove many established ideas regarding air pollution in the United States. Due to a lack of relevant data, it remains to be seen how health damage attributed to air pollution worldwide compares to that in the United States.